Delay-induced remote synchronization in bipartite networks of phase oscillators

Nirmal Punetha,[1] Sangeeta Rani Ujjwal,[2] Fatihcan M. Atay,[3] and Ramakrishna Ramaswamy[2,4]
[1]*Department of Physics and Astrophysics, University of Delhi, Delhi 110007, India*
[2]*School of Physical Sciences, Jawaharlal Nehru University, New Delhi 110067, India*
[3]*Max Planck Institute for Mathematics in the Sciences, Inselstr. 22, Leipzig 04103, Germany*
[4]*University of Hyderabad, Hyderabad 500 046, India*
(Received 11 October 2014; published 26 February 2015)

We study a system of mismatched oscillators on a bipartite topology with time-delay coupling, and analyze the synchronized states. For a range of parameters, when all oscillators lock to a common frequency, we find solutions such that systems within a partition are in complete synchrony, while there is lag synchronization between the partitions. Outside this range, such a solution does not exist and instead one observes scenarios of *remote* synchronization—namely, chimeras and individual synchronization, where either one or both of the partitions are synchronized independently. In the absence of time delay such states are not observed in phase oscillators.

DOI: 10.1103/PhysRevE.91.022922 PACS number(s): 05.45.Ac, 05.45.Pq, 05.45.Xt

I. INTRODUCTION

A wide variety of collective phenomena in nature can be studied through models of interacting dynamical units [1–5]. A common structure that has been explored in such studies is the bipartite network [6–13], namely, the situation when the system can be divided in two subsets such that units in one subset or partition *only* interact with units in the other partition and not with any unit in the same partition. Examples of such networks include units connected in a chain, stars, trees, or rings with an even number of nodes.

In any realistic experimental situation, perfectly identical systems are difficult to engineer, and thus the situation above is frequently encountered in practice. In addition to heterogeneities which arise naturally due to dissimilarities in intrinsic parameters, it is also necessary to consider heterogeneity in connection topology as well as in the coupling; these also modify the behavior of the system, affecting synchronization [14,15] or causing riddling [16] or amplitude death [17]. Time delay is inherent in the coupling when there is a finite speed in the signal propagation. It is also known that these effects can change the nature of the dynamical states quite significantly [18–20].

In the present paper we consider delay-coupled phase oscillators on a bipartite network similar to the one schematically depicted in Fig. 1, all oscillators in a partition being coupled to all oscillators in the other. Oscillators in the two partition are mismatched, namely, they have different inherent frequencies. We find that this system can exhibit both global [5] as well as *remote* synchronization (RS) [21,22]. In the former case, oscillators in both partitions lock on to a common frequency, although a phase difference between the set of oscillators in the two partitions can arise. Depending on the mismatch, namely, the difference in the inherent frequencies of the partitions, the phase difference between the oscillators in the two partitions can be either zero or can be approximately π.

Remote synchronization describes the situation where oscillators that are coupled indirectly through a relaying oscillator become phase synchronized. They are, however, unsynchronized with the relaying (or transmitting) oscillator. This form of synchrony has been discussed in detail recently for mismatched oscillators coupled without delay, and the analysis has been in terms of the *amplitude* of oscillations [21,22]. There are two manifestations of RS in this system. In the first case, oscillators in the two partitions lock on to different time-dependent frequencies causing individual synchronization of the partitions. The second form of RS is more interesting: there can be chimera states with all oscillators in one partition being phase coherent while all the oscillators in the other partition are not. Such states, with coexisting coherent and incoherent groups of oscillators, have attracted considerable attention in recent years, and have typically been seen in networks of nonlocally coupled oscillators [23,24].

In Sec. II of this paper we introduce the system of delay-coupled mismatched phase oscillators on a bipartite network, and discuss criteria for the existence of globally synchronized solutions. By examining oscillator frequencies and phase response, the behavior of the system is analyzed within these regions. Remote synchrony is discussed in Sec. III and we use the Kuramoto order parameter to identify different scenarios of remote synchronization that are observed in various regions of the parameter space. Finally, Sec. IV summarizes our main results; the possibility of RS in coupled *phase* oscillators suggests that this phenomenon has considerable generality and is thus worthy of further study.

II. PHASE OSCILLATORS ON A BIPARTITE NETWORK

The two partitions are denoted A and B, and the dynamics of the phase oscillators in each partition are determined by the evolution equations

$$\dot{\theta}_i = \begin{cases} \omega_A + \dfrac{\varepsilon}{k_i}\displaystyle\sum_{j\in B} a_{ij}\sin[\theta_j(t-\tau)-\theta_i(t)], & \text{if } i \in A \\ \omega_B + \dfrac{\varepsilon}{k_i}\displaystyle\sum_{j\in A} a_{ij}\sin[\theta_j(t-\tau)-\theta_i(t)], & \text{if } i \in B, \end{cases} \tag{1}$$

where $\theta_i(t)$ is the phase of ith oscillator at time t. There are N_A and N_B oscillators in the two partitions, and their intrinsic frequencies are ω_A and ω_B, respectively. These can be written in terms of the mean, $\bar{\omega} = (\omega_A + \omega_B)/2$, and the

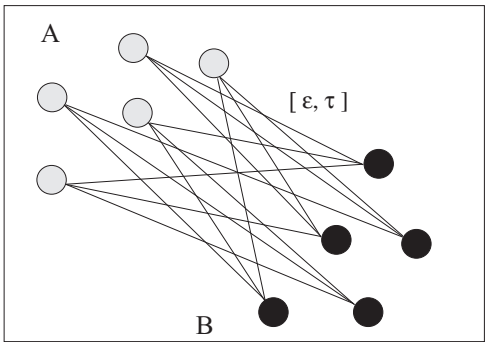

FIG. 1. Schematic diagram of the bipartite network studied here where the nodes separate into two groups denoted A and B. We consider phase oscillators at each node, with coupling of strength ε and delay τ only between oscillators belonging to different partitions or groups. In numerical calculations we have taken 32 oscillators in each partition.

mismatch $\Delta\omega/2$; $\omega_{A,B} = \bar{\omega} \pm \Delta\omega/2$. The coupling strength is ε. Elements of the adjacency matrix, $a_{ij} = 1$ if the ith and jth oscillators are connected, and zero otherwise, and $k_i = \sum_j a_{ij}$ counts the number of links to the ith oscillator.

A. Globally synchronized solutions

Global synchronization is established in a network when all the oscillators are entrained to a common frequency Ω. The solutions are given, generally, as

$$\theta_i = \begin{cases} \Omega t - \phi/2, & \text{if} \quad i \in A \\ \Omega t + \phi/2, & \text{if} \quad i \in B, \end{cases} \tag{2}$$

where ϕ is the phase difference between the partitions. Substituting this solution into Eq. (1), the condition for phase locking requires

$$\Omega = \omega_A + \varepsilon \sin(-\Omega\tau - \phi) = \omega_B + \varepsilon \sin(-\Omega\tau + \phi). \tag{3}$$

This leads to the following transcendental equation for the synchronization frequency Ω,

$$\Omega_\mp = \bar{\omega} \mp \varepsilon \tan(\Omega_\mp \tau)\sqrt{\cos^2(\Omega_\mp \tau) - (\Delta\omega/2\varepsilon)^2}, \tag{4}$$

while the phase difference ϕ between the partitions is given by

$$\phi = \begin{cases} \arcsin\left(\frac{\Delta\omega}{2\varepsilon\cos(\Omega\tau)}\right), & \text{if} \quad \cos(\Omega\tau) > 0 \\ \pi - \arcsin\left(\frac{\Delta\omega}{2\varepsilon\cos(\Omega\tau)}\right), & \text{if} \quad \cos(\Omega\tau) < 0. \end{cases} \tag{5}$$

There are two possible solutions, and the respective stability conditions are [25]

$$\cos(-\Omega\tau - \phi) > 0 \text{ and } \cos(-\Omega\tau + \phi) > 0. \tag{6}$$

For identical oscillators, when $\Delta\omega = 0$ and $\bar{\omega} = \omega$, the only possibilities are in-phase ($\phi = 0$) and antiphase ($\phi = \pi$) solutions, with corresponding frequencies given by the roots of

$$\Omega_{0,\pi} = \bar{\omega} \mp \varepsilon \sin(\Omega_{0,\pi}\tau). \tag{7}$$

The in-phase solution is stable [see Eq. (6)] when $\cos(\Omega\tau) > 0$, while the antiphase solution is stable when $\cos(\Omega\tau) < 0$ [13].

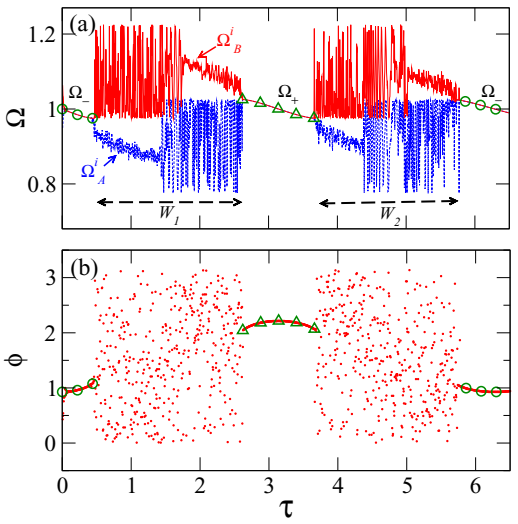

FIG. 2. (Color online) Analytically calculated plots of (a) synchronized frequencies $\Omega_\mp$, and (b) phase difference ϕ, shown with symbols (circles and triangles) as a function of delay τ, for $\Delta\omega = 0.2$ and $\varepsilon = 0.125$. Numerically obtained frequencies from the system Eq. (1) are plotted with lines (dashed blue and solid red) in (a) and the phase difference with red dots in (b).

B. Desynchronized regions

For a network of identical oscillators, it is clear that real solutions to Eq. (7) will exist for all values of ε and τ. With frequency mismatch, though, the condition

$$\cos^2(\Omega\tau) - \left(\frac{\Delta\omega}{2\varepsilon}\right)^2 \geqslant 0, \tag{8}$$

or assuming coupling strength $\varepsilon > 0$,

$$|\cos(\Omega\tau)| \geqslant \frac{|\Delta\omega|}{2\varepsilon}, \tag{9}$$

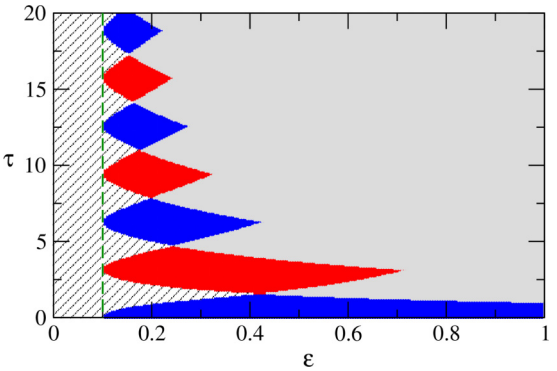

FIG. 3. (Color online) Behavior of the system in the (ε,τ) plane for a fixed frequency mismatch $\Delta\omega = 0.2$. The hatched region represents the parameter values where synchronized solutions Eq. (2) do not exist. In the blue (dark gray) region, only the solutions Ω_- are observed, and only Ω_+ frequencies are observed in the red (medium gray) region while both coexist in the multistable region shown in gray (light gray). The dashed vertical line at $\varepsilon = \Delta\omega/2 = 0.1$ is the limit below which Eq. (9) is not satisfied for any delay value.

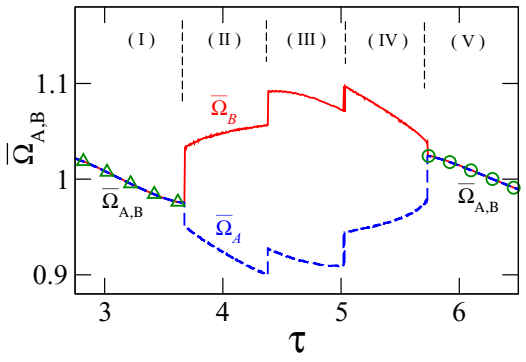

FIG. 4. (Color online) Time averaged frequencies of the oscillators from both partitions $\bar{\Omega}_A \in A$ (dashed blue) and $\bar{\Omega}_B \in B$ (solid red) are plotted as a function of the time delay τ. For regions I and V, frequencies are equal and independent of time. One partition is synchronized while the other remains incoherent in regions II and IV. In region III, both partitions are separately synchronized.

is the criteria when the transcendental equation for the collective frequency, namely, Eq. (4), has real solutions. There can, therefore, be regions in the (ε,τ) plane where solutions of the form Eq. (2) do not exist: frequency entrainment of all oscillators to a common value, and hence global synchronization, is not possible.

Figure 2 graphically displays the global behavior of an ensemble of oscillators as a function of the time delay τ. The condition Eq. (9) is satisfied over specific ranges when there is global synchrony. These can be identified as those regions where the simulation data shown matches the results of analytic estimations from Eq. (4) for the oscillator frequencies [Fig. 2(a)] and for the interpartition phase difference, plotted in Fig. 2(b). As can be seen, the analytical estimates [from Eq. (4)], namely, Ω_- (green circles) and Ω_+ (green triangles), are in excellent agreement with the numerical results [26] (see the figure caption for the details).

The portions indicated by W_1 and W_2 in Fig. 2 are regions of asynchrony, where the condition Eq. (9) is not satisfied. The oscillators in the two partitions can show two types of behavior: either near-coherence in one partition with oscillators in the other partition being incoherent, or a global lack of coherence in both partitions. In either case, the interpartition phase difference changes with time and takes arbitrary values between 0 and π [see Fig. 2(b)].

The behavior of the system as a function of coupling strength and time delay is summarized in Fig. 3 for a fixed level of mismatch in the frequencies of the uncoupled oscillators.

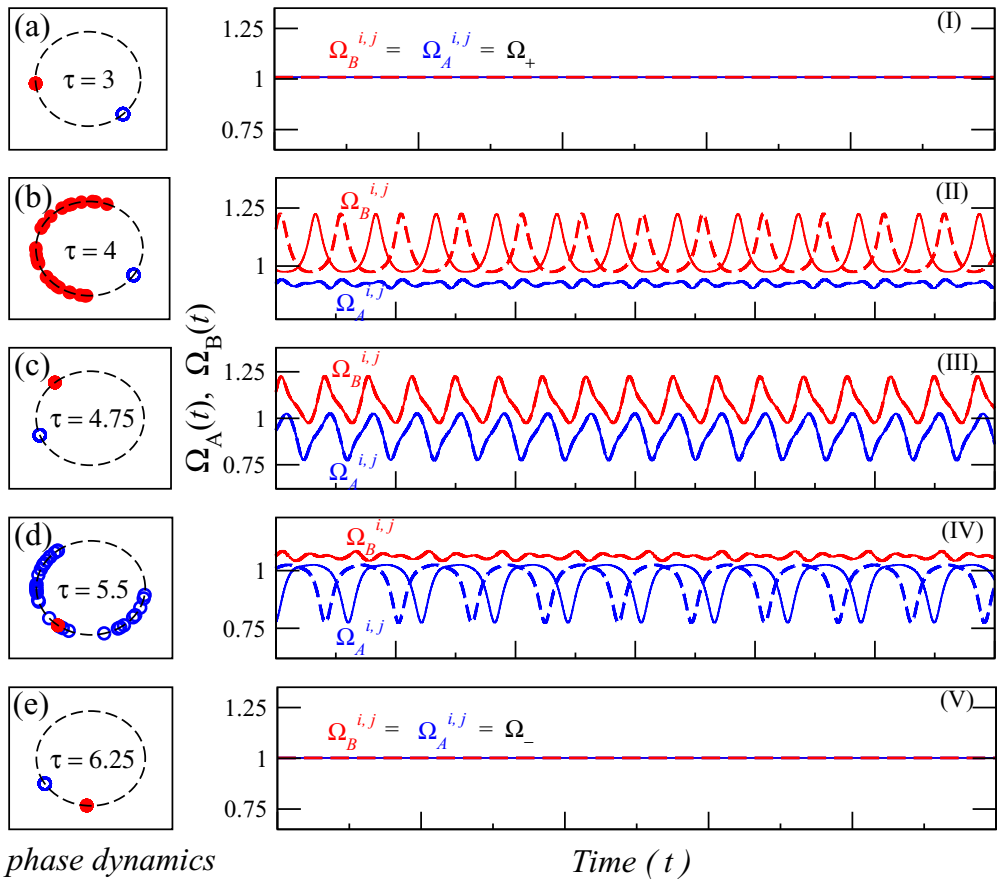

FIG. 5. (Color online) In the right panel, time variation of frequencies of four oscillators ($\Omega_A^{ij} \in A, \Omega_B^{ij} \in B$), are plotted with blue (lower) curves and red (upper) curves, respectively. The frequencies of the two chosen oscillators from each partition is shown with solid and dashed lines. The corresponding phase dynamics is plotted in the left panel. The frequencies for the two partitions are equal and constant in time for (a) and (e). (b) and (d) indicate chimeras, as only one of the partitions is locked to a time dependent frequency while the other partition is phase incoherent. In (c), the oscillators in both partitions are separately synchronized.

In the hatched area, synchronized solutions cannot exist, and this region grows in size with increasing mismatch. The colored regions (blue, red, and gray) have at least one stable synchronized solution, with the solution corresponding to Ω_- being stable in the blue region, Ω_+ in the red region, and both being stable in the gray region.

The width of desynchronized windows W_1 and W_2 can be controlled by varying the ratio $\Delta\omega/2\varepsilon$. We observe that these windows disappear for small mismatch and high coupling strengths. Increasing the ratio $\Delta\omega/2\varepsilon$ leads to the larger gaps, and when $|\Delta\omega| > 2\varepsilon$ no globally synchronized solution is possible in the system for any delay (see dashed vertical line in Fig. 3).

III. TIME-DEPENDENT FREQUENCIES AND REMOTE SYNCHRONIZATION

In the asynchronous region, the general form of the solution for the system Eq. (1) can be written as

$$\theta_i(t) = G_i(t) + c_i, \tag{10}$$

where G_i is a nonlinear function of time and c_i is the time-independent part. (In the synchronized regime, by contrast, $G_i(t) = \Omega t$ and the collective frequency Ω is constant in time). The frequencies, which are given by $\dot{\theta}_i(t) = \dot{G}_i(t)$, are such that their time averages are the same for all oscillators within a partition, namely,

$$\langle \dot{G}_i(t) \rangle = \begin{cases} \bar{\Omega}_A, & \text{if} \quad i \in A, \\ \bar{\Omega}_B, & \text{if} \quad i \in B. \end{cases} \tag{11}$$

A typical result is shown in Fig. 4 for $\Delta\omega = 0.2$ and $\varepsilon = 0.125$, with $\bar{\Omega}_A \in A$ (dashed-blue line) and $\bar{\Omega}_B \in B$ (solid-red lines) plotted as a function of the time delay τ. Five regions are indicated: in regions I and V, there is global synchrony, $\bar{\Omega}_A$, $\bar{\Omega}_B$ are equal and match the analytical frequencies, namely, the roots of Eq. (4), $\bar{\Omega}_A = \bar{\Omega}_B = \Omega$. In regions II, III, and IV, where Eq. (4) has no roots, then we have equal intrapartition and different interpartition average frequencies ($\bar{\Omega}_A \neq \bar{\Omega}_B$), leading to the bubblelike structures in Fig. 4. There are abrupt transitions in the average frequencies between these regions, though, corresponding to different types of coexisting states in the two partitions.

These different states are depicted in Fig. 5. The time-dependent behavior of the frequencies is shown in the right panel, along with the phases in the left panel. Frequencies of two randomly selected oscillators from both partitions are plotted in blue (lower) and red (upper) curves, indicated by $\Omega_A^{i,j}$ and $\Omega_B^{i,j}$, respectively. Regions I and V of Fig. 4 correspond to Figs. 5(a) and 5(e), and here the frequencies of all oscillators in the network are equal and constant in time; this is the globally synchronized state. In region II [panel (b)], region III [panel (c)], and region IV [panel (d)], the frequencies are time dependent and unequal for the two partitions. For the delay corresponding to Fig. 5(c), the frequencies of the oscillators in each partition are equal but time dependent, and thus each partition is separately synchronized, but $\Omega_A(t) \neq \Omega_B(t)$. For other values of the delay, there are chimeras—see Figs. 5(b) and 5(d)—with oscillators in one partition locked to a common (but time-dependent) frequency, while the oscillators in the other partition are phase incoherent, although they all have similar time-dependent frequencies.

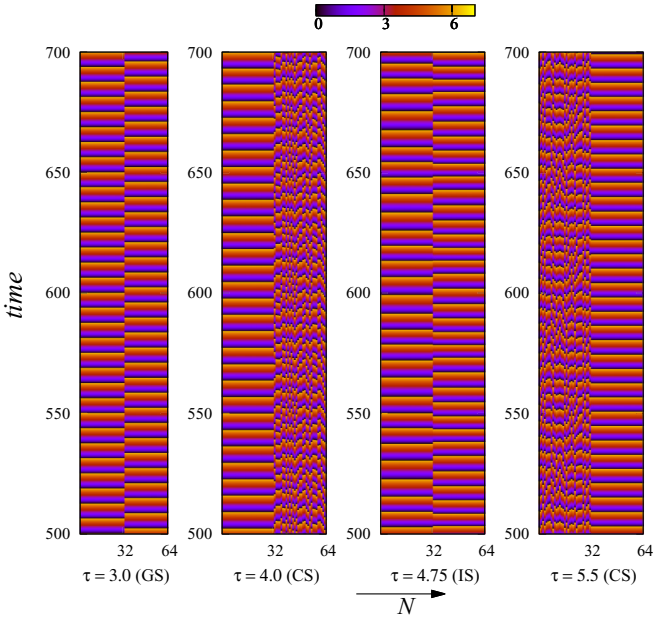

FIG. 6. (Color online) Time evolution of oscillator phases at four different delay values ($N = 64$). When $\tau = 3.0$, both partitions are globally synchronized (GS) with equal frequencies and have a nonzero phase difference. For $\tau = 4.0$ and 5.5, we see chimera states (CS) where only one of the partitions is synchronized. Individual synchronization (IS) is observed for $\tau = 4.75$ wherein both partitions are independently synchronized.

The dynamics in regions II, III, and IV in Figs. 4 and 5 are instances of *remote* synchronization where one, or separately, both partitions are synchronized. Synchronization in these regions share the feature that the phases are locked even if the frequencies are not constant in time. Since the oscillators within a partition are not coupled to each other, this synchronization is induced by the other partition which itself may not be synchronized. The time evolution diagrams of oscillator phases corresponding to different behaviors in these regions are shown in Fig. 6. With the variation in delay, transitions between these behaviors are accompanied

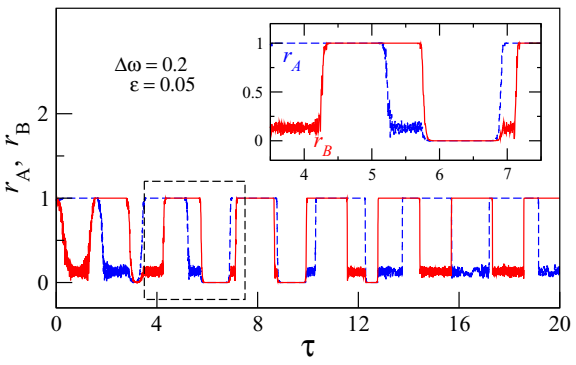

FIG. 7. (Color online) Variation of the real parts r_A and r_B of the partition order parameters as a function of the time delay τ.

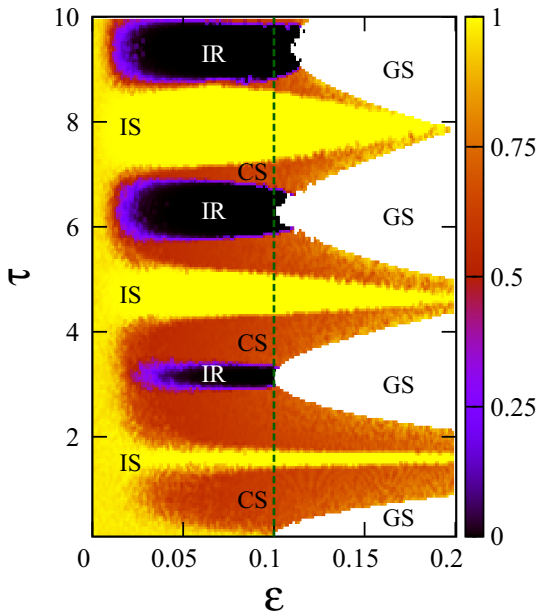

FIG. 8. (Color online) Level sets of the order parameter r as a function of ε and τ, demarcating the regions of different scenarios of remote synchronization. Red regions (CS) indicate chimera states ($r \approx 0.5$), and yellow regions (IS) are where both the partitions are independently synchronized ($r \approx 1$). In black regions (IR) oscillators in both the partitions move incoherently ($r \approx 0$). Blank white regions (GS) represent globally synchronized solutions Eq. (2). The vertical dashed line at $\varepsilon = \Delta\omega/2 = 0.1$ indicates the threshold for the existence of GS solutions.

by a discontinuous change in time averaged frequencies of individual partitions (see Fig. 4).

Partition order parameters

It is natural to use the well-known complex order parameter [5] defined in each partition, namely,

$$z_A = r_A e^{\iota\psi_A} = \frac{1}{N_A}\sum_{j\in A} e^{\iota\theta_j}, \tag{12}$$

$$z_B = r_B e^{\iota\psi_B} = \frac{1}{N_B}\sum_{j\in B} e^{\iota\theta_j}, \tag{13}$$

in order to distinguish the different dynamical behaviors of the system in the regions where synchronized solutions, namely, of the form Eq. (2), do not exist. The real parts $r_{A,B}$ of the complex order parameters measure the coherence, values close to 1 indicating that the oscillators within a partition are synchronized. Here we focus upon the real parts only since the average phases $\psi_{A,B}$ show irregular variations as a function of coupling parameters and hence do not carry much information about the coherence.

A typical result is shown in Fig. 7 for the parameter values $\Delta\omega = 0.2$ and $\varepsilon = 0.05$, where the variation of the real parts r_A (dashed-blue line) and r_B (solid-red lines) are plotted as a function of delay. In a chimeric state when one of the partitions is synchronized and the other is out of sync, then one of r_A or r_B is ≈ 1 while the other is around 0. In a scenario when both partitions are individually synchronized (region III in Fig. 4), both r_A and r_B are near 1. Similarly

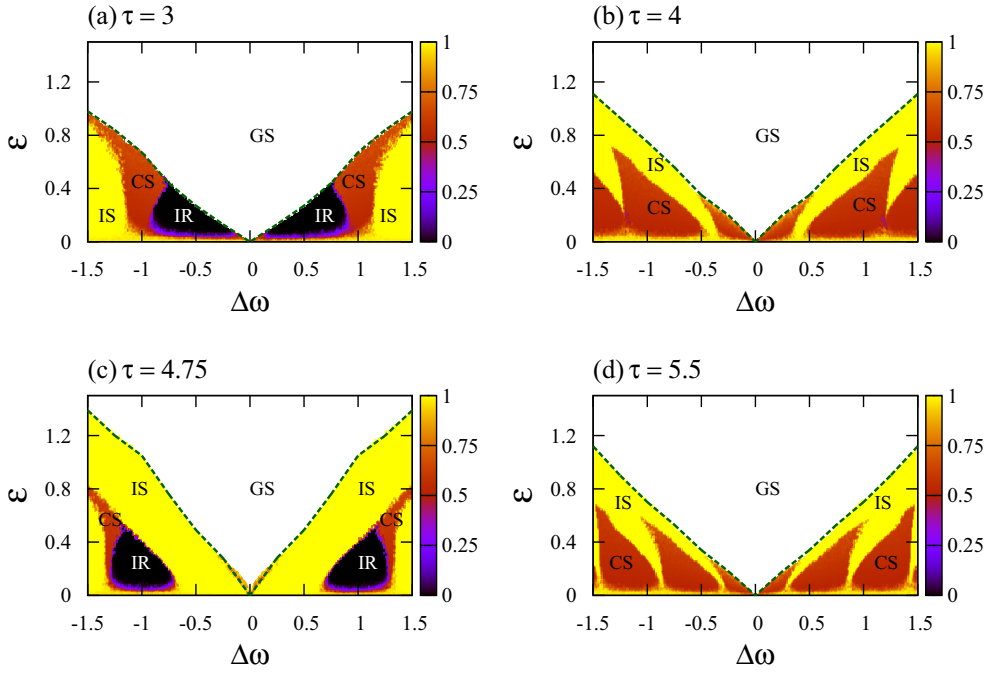

FIG. 9. (Color online) Similar to Fig. 8 for different τ values, as a function of $\Delta\omega$ and ε. The blank white regions (GS) show global synchronization. Red regions (CS) indicate chimera state ($r \approx 0.5$), and yellow regions (IS) represent when both the partitions are individually synchronized ($r \approx 1$). In the black regions (IR) oscillators in both the partitions move incoherently ($r \approx 0$). The dashed curves show the boundary below which globally synchronized solutions disappear.

there is also the case when both r_A and r_B are approximately 0, indicating incoherent behavior in both partitions. These different states are clearly visible in the figure and inset. In these regions one can also use the average $r = (r_A + r_B)/2$ to characterize the state. $r \approx 0.5$ for a chimera (CS), and $r = 1$ indicates a separate synchronization of both partitions (IS) while $r \approx 0$ represents incoherent behavior in both partitions (IR).

This quantity is shown in Fig. 8 as a function of the coupling ε and the delay τ for fixed mismatch $\Delta\omega = 0.2$, and in Fig. 9 for different delays as a function of coupling and mismatch. In both we observe chimeras (the red regions where $r \approx 0.5$), individual synchronization of the partitions (the yellow regions where $r \approx 1$), and incoherent behavior (the black regions with $r \approx 0$). The blank region in Fig. 9 shows the "Arnold tongue" of globally synchronized solutions, given by the criterion Eq. (9) with the collective frequency Ω being estimated as the root of the transcendental equation, Eq. (4).

IV. SUMMARY AND DISCUSSION

Delay-coupled phase oscillators on a bipartite network show interesting and novel collective states. In addition to global synchrony when all the oscillators in the network lock onto a common frequency, there can also be *remote* synchronization, with different groups of indirectly connected oscillators displaying distinct patterns of phase coherence.

For these effects to occur, both the time-delay coupling as well as the bipartite topology appear to be important. Coupled phase oscillators in the absence of time delay do not show remote synchrony, and oscillators with local coupling but without the bipartite topology have not hitherto been known to support chimera states. Some analysis is possible in the present system, and we are able to obtain a criterion for global synchronization. We also locate regions in parameter space where remote synchronization occurs.

In these latter regions, namely, when there is RS, a delicate balance must be achieved [21]. Since the oscillators that synchronize are not directly connected, and they remain unsynchronized with the mediating unit(s), remote synchronization depends upon the frequency mismatch, on the network topology, and also on the behavior of perturbations in the relaying units. The mismatch between the frequencies must be such that the oscillators that are coupled indirectly may synchronize while avoiding frequency locking with the relaying unit(s). Furthermore, the perturbations should not decay rapidly in the relaying oscillators [21]. The introduction of time delay achieves this and hence we find remote synchronization even for phase oscillators. Note that RS observed here is different from the symmetry-induced phase synchronization in a network of identical oscillators where all the oscillators lock to a common frequency [27].

A number of natural systems have the bipartite topology, and significant delays also arise frequently in situations where signals propagate with a finite velocity. Thus the present results are likely to be fairly general. Qualitatively similar results are obtained when the oscillator frequencies of both partitions are drawn from Gaussian distributions with different means and variances [28]. The occurrence of RS in a system of delay-coupled phase oscillators suggests that these results may have wider implications for neuroscience, brain research, climate research, and other fields that involve delayed information transmission [21,27,29].

ACKNOWLEDGMENTS

N.P. and R.R. thank the Department of Science and Technology, India. S.R.U. acknowledges the CSIR, India, for support from the award of a Senior Research Fellowship. F.M.A. acknowledges the support of the European Union's Seventh Framework Programme (FP7/2007-2013) under Grant Agreement No. 318723 (MatheMACS).

[1] S. H. Strogatz, Nature (London) **410**, 268 (2001).
[2] E. Schöll, Nat. Phys. **6**, 161 (2010).
[3] R. Albert and A.-L. Barabasi, Rev. Mod. Phys. **74**, 47 (2002).
[4] A. T. Winfree, *The Geometry of Biological Time* (Springer, New York, 1980).
[5] Y. Kuramoto, *Chemical Oscillations, Waves and Turbulence* (Springer-Verlag, Berlin, 1984).
[6] H. Jeong, B. Tombor, R. Albert, Z. N. Oltvai, and A.-L. Barabási, Nature (London) **407**, 651 (2000).
[7] M. E. J. Newman, Proc. Natl. Acad. Sci. U.S.A. **98**, 404 (2001).
[8] P. Holme, F. Liljeros, C. R. Edling, and B. J. Kim, Phys. Rev. E **68**, 056107 (2003).
[9] J. Ohkubo, K. Tanaka, and T. Horiguchi, Phys. Rev. E **72**, 036120 (2005).
[10] J. L. Guillaume and M. Latapy, Phys. A (Amsterdam, Neth.) **371**, 795 (2006).
[11] S. Saavedra, F. R. Tsochas, and B. Uzzi, Nature (London) **457**, 463 (2009).
[12] K. Sneppen, M. Rosvall, A. Trusina, and P. Minnhagen, Europhys. Lett. **67**, 349 (2004).
[13] N. Punetha, R. Ramaswamy, and F. M. Atay (unpublished).
[14] H. Hong and S. H. Strogatz, Phys. Rev. Lett. **106**, 054102 (2011).
[15] G. A. Johnson, D. J. Mar, T. L. Carroll, and L. M. Pecora, Phys. Rev. Lett. **80**, 3956 (1998).
[16] S. Yanchuk and T. Kapitaniak, Phys. Rev. E **68**, 017202 (2003).
[17] K. Bar-Eli, Phys. D (Amsterdam, Neth.) **14**, 242 (1985); R. E. Mirollo and S. H. Strogatz, J. Stat. Phys. **60**, 245 (1990); G. B. Ermentrout, Phys. D (Amsterdam, Neth.) **41**, 219 (1990).
[18] H. G. Schuster and P. Wagner, Prog. Theor. Phys. **81**, 939 (1989).
[19] M. Lakshmanan and D. V. Senthilkumar, *Dynamics of Nonlinear Time-Delay Systems* (Springer-Verlag, Berlin, 2011); *Complex Time-Delay Systems*, edited by F. M. Atay (Springer-Verlag, Berlin, 2010); W. Just, A. Pelster, M. Schanz, and E. Schöll, Phil. Trans. R. Soc. A **368**, 301 (2010).
[20] D. V. Ramana Reddy, A. Sen, and G. L. Johnston, Phys. Rev. Lett. **80**, 5109 (1998); F. M. Atay, *ibid.* **91**, 094101 (2003); I. Fischer *et al.*, *ibid.* **97**, 123902 (2006); G. Saxena, A. Prasad, and R. Ramaswamy, Phys. Rev. E **82**, 017201 (2010).

[21] A. Bergner, M. Frasca, G. Sciuto, A. Buscarino, E. J. Ngamga, L. Fortuna, and J. Kurths, Phys. Rev. E **85**, 026208 (2012).

[22] L. V. Gambuzza, A. Cardillo, A. Fiasconaro, L. Fortuna, J. Gómez-Gardeñes, and M. Frasca, Chaos **23**, 043103 (2013).

[23] Y. Kuramoto and D. Battogtokh, Nonlinear Phenom. Complex Syst. (Minsk, Belarus) **5**, 380 (2002); D. M. Abrams and S. H. Strogatz, Phys. Rev. Lett. **93**, 174102 (2004); C. R. Laing, Phys. D (Amsterdam, Neth.) **238**, 1569 (2009).

[24] G. C. Sethia, A. Sen, and F. M. Atay, Phys. Rev. Lett. **100**, 144102 (2008); J. H. Sheeba, V. K. Chandrasekar, and M. Lakshmanan, Phys. Rev. E **79**, 055203R (2009).

[25] F. M. Atay, Phil. Trans. R. Soc. A **371**, 20120460 (2013).

[26] The delay differential equation Eq. (1) is solved using forth order Runge–Kutta method with integration step $= \tau/D$. Discreteness $D = 700$. We consider the system of 64 oscillators, $N_A = N_B = 32$, and $\bar{\omega} = 1.0$. However the results have been verified for different network sizes $N = 16,32$, and 128. All quantities (frequencies and phases) are calculated after removing the appropriate number of transients.

[27] V. Nicosia, M. Valencia, M. Chavez, A. Diaz-Guilera, and V. Latora, Phys. Rev. Lett. **110**, 174102 (2013).

[28] We have studied the case when the frequencies of oscillators in each partition are drawn from two Gaussian distributions with mean values $\mu_{1,2} = \bar{\omega} \pm \Delta\omega$ and variance $\sigma = \Delta\omega/(2 \times 10^2)$. Note that for a very large variance there can be significant effects since the condition required for remote synchronization will also fail.

[29] J. F. Donges, Y. Zou, N. Marwan, and J. Kurths, Europhys. Lett. **87**, 48007 (2009); D. Maraun and J. Kurths, Geophys. Res. Lett. **32**, L15709 (2005).